Solution routes to lead titanate: synthesis, molecular structure and reactivity of the Pb–Ti and Pb–Zr species formed between various lead oxide precursors and titanium or zirconium alkoxides. Molecular structure of $Pb_2Ti_2(\mu_4\text{-}O)(OAc)_2(OPr^i)_8$ and of $PbZr_3(\mu_4\text{-}O)(OAc)_2(OPr^i)_{10}$

Liliane G. Hubert-Pfalzgraf,*[a] Stéphane Daniele,[a] Renée Papiernik,[a] Marie-Cécile Massiani,[a] Bernard Septe,[a] Jacqueline Vaissermann[b] and Jean-Claude Daran[b]

[a]*Laboratoire de Chimie Moléculaire, URA-CNRS, Université de Nice-Sophia-Antipolis, Parc Valrose, 06108 Nice Cédex 2, France*

[b]*Laboratoire de Chimie des Métaux de Transition, URA-CNRS, 75 230 Paris Cédex 5, France*

The reactions between $Ti(OR)_4$ (R = Et, Pr^i) or $[Zr(OPr^i)_4(Pr^iOH)]_2$ and various lead oxide precursors [anhydrous $Pb(OAc)_2$, alkoxides or oxoalkoxides] have been investigated in different experimental conditions (solvent, temperature). Various mixed-metal species have been isolated in high yields and characterized by microanalysis, FTIR and multinuclear NMR (^1H, ^{13}C and ^{207}Pb) spectroscopies. The mixed-metal oxoacetatoalkoxides $Pb_2Ti_2(\mu_4\text{-}O)(\mu\text{-}OAc)_2(\mu\text{-}OPr^i)_5(OPr^i)_3$ **1** and $PbZr_3(\mu_4\text{-}O)(\mu\text{-}OAc)_2(\mu\text{-}OPr^i)_5(OPr^i)_5$ **2** have been characterized by X-ray crystallography at −100 °C: for **1**, monoclinic, space group C_2/c with $a = 38.916(17)$ Å, $b = 12.045(2)$ Å, $c = 19.046(4)$ Å, $\beta = 112.84(3)°$, $V = 8224(4)$ Å^3, $Z = 8$, $R = 0.068$, $R_w = 0.076$; and for **2**, monoclinic, space group $P2_1/n$ with $a = 10.618(2)$ Å, $b = 25.157(11)$ Å, $c = 18.611(5)$ Å, $\beta = 90.35(2)°$, $V = 4971(3)$ Å^3, $Z = 4$, $R = 0.060$, $R_w = 0.072$. Hydrolysis–condensation reactions have been achieved especially for the species having a Pb : Ti stoichiometry appropriate for access to $PbTiO_3$. Effects of the solvent on the temperature of crystallisation and on the particle size are discussed.

Ferroelectric materials based on the perovskite structure are of great interest in microelectronics finding applications in pyroelectric and piezoelectric devices, actuators, sensors, non-volatile memories and optical waveguides.[1] Lead titanate $PbTiO_3$ (PT) and $Pb(Zr_{1-x}Ti_x)O_3$ (PZT) are well known ferroelectrics. Chemical routes, especially sol–gel processing, offer advantages over physical deposition techniques and have attracted wide interest. Solution routes require soluble compounds and various precursors, based either on homometallic species or on heterometallic ('single source') precursors, have been used.[2,3] Cohydrolysis of lead acetate trihydrate and various zirconium and titanium derivatives (alkoxides, acetylacetonatoalkoxides) has been studied extensively for wet chemical routes to PZT.[3–6] Different solvents (parent alcohol, 2-methoxyethanol,[4,5] diols[6]) have been evaluated for simultaneous control of the homogeneity, the hydrolysis rates and/or the rheology. While lead acetate trihydrate has been most widely used, lead alkoxides, formulated as $Pb(OR)_2$ and stabilized by monoethanolamine,[7] or functional carboxylates, either glycolate or dimethylglycolate, are alternative sources of lead oxide. The latter have been selected for the control of the 1 : 1 stoichiometry between lead and titanium [as $Ti(OPr^i)_4$[8] or $Ti(OPr^i)_2(acac)_2$[9]] but the poor solubility of the Pb–Ti species formed precluded unequivocal characterization. Formation of crystalline single-phase materials at low temperatures is desired for thin film applications. These features might depend on the nature of the initial precursors: mixture of homometallic species, mixed-metal derivatives, nature of the ligands, of the additives, but knowledge of the chemical processes remains limited.

The composition of the precursor solutions has generally been investigated by FTIR[6,10] and NMR spectroscopies, and sometimes by mass spectrometry.[11] EXAFS has been used for understanding the first steps of the polycondensation process.[12] The presence of various Pb–Ti species, especially $PbTiO_2(OR)_2$, has thus been postulated.[3,11] $Pb_2Ti_2(\mu_4\text{-}O)(OPr^i)_{10}$[13a] and $Pb_2Ti_4(\mu_4\text{-}O)(OAc)_2(\mu\text{-}OEt)_6(OEt)_8$[1,14,15] are, however, the only structurally characterized lead–titanium species reported so far. Regarding lead–zirconium species, $Pb_2Zr_4(\mu_4\text{-}O)_2(OAc)_4(OEt)_{12}$ has recently been reported,[16] while the formation of $PbZr_3O(OAc)_2(OPr^i)_{10}$ was indicated by us in a conference proceedings communication.[17]

In order to obtain a better insight into the relationships between the initial precursor and the final material, we have investigated the nature of the species obtained by reacting lead alkoxides or lead acetate with various titanium and zirconium alkoxides under different experimental conditions (alkoxide ligands, solvent, temperature, order of addition of the reagents, *etc.*). Various mixed-metal species have been isolated, characterized by elemental analysis, FTIR (Table 1) and multinuclear NMR (^1H, ^{13}C, ^{207}Pb) spectroscopy (Table 2). $Pb_2Ti_2O(OAc)_2(OPr^i)_8$ **1** and $PbZr_3O(OAc)_2(OPr^i)_{10}$ **2** were also characterized by single-crystal X-ray diffraction. Their conversion into oxides by hydrolysis–polycondensation reactions has been achieved. Hydrolysis intermediates have been isolated for $Pb_2Ti_2O(OAc)_2(OPr^i)_8$.

Experimental

Manipulations were performed under dry nitrogen using standard Schlenk-tube and vacuum-line techniques with solvents purified by standard methods. Anhydrous lead acetate was obtained by refluxing the hydrate, $Pb(OAc)_2\cdot 3H_2O$, in acetic anhydride and titanium alkoxides were distilled *in vacuo.* $[Pb(OPr^i)_2]_\infty$, $Pb_4O(OPr^i)_6$, $Pb_4O(OEt)_4$,[18] $[Zr(OPr^i)_4(Pr^iOH)]_2$[19] and $Pb_2Ti_2O(OPr^i)_{10}$[13a] were synthesized as reported in the literature. NMR spectra were recorded on a Bruker AC-200 spectrometer at 200.13 (^1H), 50.32 (^{13}C) or 41.75 MHz (^{207}Pb). The lead chemical shifts are quoted with respect to $Pb(NO_3)_2$ in D_2O as an external reference and are positive to low field. IR spectra were run on a IR-FTS 45 spectrometer and were obtained as Nujol mulls between KBr plates for the air-sensitive compounds, and as KBr pellets for the powders resulting from hydrolyses. Analytical data were obtained from the Centre de Microanalyses du CNRS.

Hydrolyses were achieved at room temperature in thf, in the parent alcohol or in parent alcohol–acetone mixture; water

Table 1 IR data for mixed-metal Pb–M compounds (M = Ti, Zr)

	IR	
compound	$\nu_{as}(CO)$, $\nu_s(CO)/cm^{-1}$	$\nu(M–OZ)^a/cm^{-1}$
$Pb_2Ti_2O(OAc)_2(OPr^i)_8$ **1**	1576s, 1553s, 1442s, 1409s	663m, 644m, 594s, 526s, 493s, 473s, 436s
$PbZr_3O(OAc)_2(OPr^i)_{10}$ **2**	1610s, 1594s, 1573s, 1456s, 1420s, 1377s	657m, 617m, 582m, 556s, 535m, 520m, 500m, 481s, 466s, 436m, 426m
$Pb_2Ti_2O(OPr^i)_{10}$ **3**	—	677w, 617s, 597s, 565s, 487sh, 471m, 420w
$[PbTi_2O(OEt)_8]_m$ **4**	—	582s, 542, 430s
$Pb_2Ti_2O(acac)_2(OPr^i)_8$ **5**	1590s, 1522s, 1457s, 1388s	658m, 607m, 582s, 508s, 470s, 407s, 357s
$Pb_4Ti_4O_6(OAc)_4(OPr^i)_8$ **6**	1545s, 1543s, 1375s, 1333s	667m, 644m, 609s, 582s, 537s, 524s, 505s, 474s, 436m, 413s

[a] Z = R, C(O)Me or C(Me)C(O)Me.

was added *via* the same solvent. Powder X-ray diffraction data were collected at variable temperatures using Cu-Kα radiation. Thermogravimetric analyses were performed on a Setaram system under nitrogen and with a heating rate of 5 °C min^{-1}. Particle sizes were estimated by sedimentation measurement (Model Capa 500 analyzer, Horiba, Ltd., Tokyo, Japan) or by light scattering (Coulter).

$Pb_2Ti_2O(OAc)_2(OPr^i)_8$ 1

$Ti(OPr^i)_4$ (8ml, 26.88 mmol) was added to a suspension of $Pb(OAc)_2$ (2.76 g, 8.48 mmol) in 40 ml of hexane. The suspension was stirred at room temperature for 72 h. After filtration and concentration of the filtrate, **1** was obtained at 5 °C; yield (1.4 g) 68%/$Pb(OAc)_2$. Anal. Calc. for $C_{28}H_{62}O_{13}Pb_2Ti_2$: C, 30.1; H, 5.6; Pb, 37.6; Ti, 8.7. Found: C, 29.8; H, 5.4; Pb, 36.9; Ti, 9.2%. Spectral characteristics as reported previously.[13a]

$PbZr_3O(OAc)_2(OPr^i)_{10}$ 2

A solution of $[Zr(OPr^i)_4(HOPr^i)]_2$ (3 g, 3.87 mmol) in hexane (30 ml) was added to a suspension of $Pb(OAc)_2$ (0.45 g, 1.38 mmol) in the same solvent. Dissolution occurred rapidly and after 24 h, the solvent was removed. Extraction with light petroleum, concentration and cooling to 5 °C afforded crystals of **2**, yield (2 g) 65%/$Pb(OAc)_2$. Anal. Calc. for $C_{34}H_{76}O_{15}PbZr_3$: C, 33.84; H 6.35. Found: C, 33.52; H, 6.22%.

$Pb_2Ti_4O_2(OAc)_2(OEt)_{14}$

1.35 g (4.15 mmol) of $Pb(OAc)_2$ was added to a solution of 2.93 g (12.8 mmol) of $Ti(OEt)_4$ in toluene and dissolved at room temperature after a few minutes. Concentration and addition of ethanol resulted in crystallisation of $Pb_2Ti_4O_2(OAc)_2(OEt)_{14}$ [2.09 g, 68%/$Pb(OAc)_2$]. Anal. Calc. for $C_{28}H_{68}O_{14}Pb_2Ti_4$: C, 27.18; H, 5.54; Pb, 33.65; Ti, 15.51. Found: C, 26.85; H, 5.45; Pb, 33.40; Ti, 15.60%. $^{207}Pb\{^1H\}$ NMR ($CDCl_3$, 20 °C) δ 2900. Other spectral characteristics as reported.[14]

The same product was obtained quantitatively by reacting $[PbTi_2O(OEt)_8]_m$ with dilute acetic acid (1 : 1 stoichiometry) in toluene at room temperature.

$[PbTi_2O(OEt)_8]_m$

1.47 g (1.32 mmol) of $Pb_4O(OEt)_6$ was added to a solution of 2.7 g (11.8 mmol) of $[Ti(OEt)_4]_m$ in 50 ml of toluene. Dissolution of the lead oxoethoxide was observed immediately at room temperature. The reaction medium was concentrated, addition of ethanol (2 ml) and cooling to −20 °C afforded crystallisation of 2.8 g of product [yield 78%/$Pb_4O(OEt)_6$]. Anal. Calc. for $C_{16}H_{40}O_9PbTi_2$: C, 28.28; H, 5.89; Pb, 30.49; Ti, 14.11. Found C, 28.5; H, 6.1; Pb, 29.5; Ti, 13.6%.

$Pb_4Ti_4O_6(OAc)_4(OPr^i)_8$

8 mg (0.45 mmol) of H_2O in 20 ml of toluene was added to a solution of 0.5 g (0.45 mmol) of $Pb_2Ti_2O(OAc)_2(OPr^i)_8$ in 25 ml of toluene. After 15 h at room temperature, the solvent was removed. The yellowish solid obtained was dissolved in light petroleum; cooling to −20 °C afforded yellowish crystals (0.36 g, yield 88%). Anal. Calc. for $C_{32}H_{68}O_{22}Pb_4Ti_4$: C, 21.0; H, 3.7; Pb, 45.4; Ti, 10.5. Found: C, 21.35; H, 3.75; Pb, 45.6; Ti, 10.7%.

The same product was obtained by addition of 0.5 equivalent of H_2O in toluene at room temperature but in lower yield (33%).

All compounds were soluble in common organic solvents. Solubilisation was generally slow in the parent alcohol.

X-Ray structure analysis of 1 and 2

X-Ray quality crystals of **1** and **2** were obtained by recrystallisation from hexane and ligroin solutions respectively at *ca.* 5 °C. Intensity data were collected at −100 °C on a Enraf-Nonius CAD4 diffractometer using Mo-Kα radiation. Crystal data and other pertinent information are listed in Table 3. Accurate cell dimensions and the orientation matrix were obtained from least-squares refinements of the setting angles of 25 well defined reflections. No decay in the intensities of three standard reflections was observed during data collection. The usual corrections for Lorentz and polarization effects were applied.

Computations were performed by using SHELXS and CRYSTALS[20] adapted on a Microvax-II computer. Scattering factors and corrections for anomalous dispersion were taken from ref. 21. Solution of the structure of **2** was accomplished by standard Patterson–Fourier techniques. An empirical absorption correction was applied (DIFABS).[22] All non-hydrogen atoms except O(15) were refined anisotropically. Constraints were applied to some C—C bond lengths and angles [around C(8), C(20), C(23) and C(32)]. All hydrogen atoms were introduced in calculated positions and their coordinates calculated after each cycle. They were allocated an isotropic thermal parameter 20% higher than that of the bonded carbons.

Parameters of the unit cell of compound **1** are: a = 38.916(17) Å, b = 12.045(2) Å, c = 19.046(4) Å, β = 112.84°, V = 8228(4) A^3. The crystal structure resolution was performed in the monoclinic space group $C2/c$ (Z = 8). One of the two Pb atoms appeared with low intensity compared to the other. After refinement, the thermal parameter value for this Pb atom was unreasonably large. This problem was solved by the introduction of two different crystallographic sites for this atom, namely Pb(2) and Pb(3) with 0.56 and 0.44 occupancy respectively. Surprisingly, all bridging and terminal O atoms were well located, even those linked to the disordered lead atom. All isopropyl groups were also well defined, except for the group linked to O(9) on the disordered lead atom which could not be located on a difference Fourier map. Refinement of the structure was carried out using 1975 reflections with $I > 3\sigma(I)$. The residuals were $R = 0.067$ and $R_w = 0.076$ with anisotropic thermal parameters for Pb and Ti atoms and isotropic thermal parameters for all other atoms. It should be noted that disorder problems related to lead centres were also observed for $Pb_2Ti_2O(OPr^i)_{10}$.[13a] Atomic coordinates, thermal

Table 2 NMR (^{1}H, ^{13}C{^{1}H}, ^{207}Pb) data for mixed-metal Pb–M compounds (M = Ti, Zr)

		NMR						
			δ(^{1}H)			δ(^{13}C)[b]		
compound	T/°C	δ(^{207}Pb)[a]	CH_3 (Ac, acac)	CH_2 (Et), CH (Pr^i, acac)	CH_3 (Et, Pr^i)	C=O (Ac, acac)	CH_2 (Et), CH (Pr^i, acac)	CH_3 (R, Ac, acac)
1	20	3016	1.95 (s, 3H)	5.05 (m, 2.4H), 4.49 (spt, 1.8H)	1.24 (d, 24H)	179.1	77.3, 76.4	26.5, 25.4
	−50	—	2.07, 1.97, 1.94 (s, 1:1:2, 12H)	5.17, 4.90 (m, 4:3, 14H), 4.73, 4.49 (q, 2:3, 10H)	1.20–1.17 (d, 24H)[c]	—	—	—
2	20	2558	1.94, 1.90 (1:1, 6H)	5.19, 4.62, 4.35 (2:5:3, 10H)	1.22–1.34 (d, 60H)[a]	180.1, 177.6	73.0, 71.5, 71.0, 70.5, 69.8, 68.5	27.5, 27.0, 26.5, 25.5, 25.0, 24.5
	−50	—	2.00, 1.95 (1:1, 6H)	5.15, 4.85, 4.65, 4.45, 4.25 (spt, 1:1:2:3:3, 10H)	1.50–1.10 (d, 60H)[c]	—	—	—
3	20	3870	—	5.10, 4.70 (m, 2:1, 6H), 4.53 (spt, 4H)	1.24 (d, 60H)	—	77.3, 76.1, 75.0	27.6, 27.0, 24.6
4	20	2560	—	4.50, 4.37 (q, 1:3, 8H)	1.20–1.40 (t, 12H)	—	68.8, 68.0, 66.2	20.5, 20.3, 19.5
	−40	—	—	4.45, 4.33, 4.02 (q, 1:2:1, 8H)	1.28–1.33 (t, 12H)[c]	—	—	—
5	20	3883	2.03, 1.92 (s, 1:1, 12H)	5.51 (s, 2H); 4.78, 4.50, 4.04 (spt, 3:1:4, 8H)	1.21 (d, 48H)	190.1	102.6, 78.7, 77.7, 64.4	26.6, 25.4, 25.1
6	20	2847	1.95 (s, 12H)	5.08, 4.87 (m, 3:2, 5H), 4.50 (q, 3H)	1.17 (d, 30H)	179.6, 178.3	72.5, 65.7	26.2
	−50	—	2.02, 1.97, 1.91 (s, 1:1:2, 12H)	5.12, 4.83, 4.72 (m, 2:2:1, 5H), 4.44 (q, 3H)	1.25–1.10 (d, 30H)[c]	—	—	—

s = Singlet, d = doublet, q = quartet, spt = septet, m = multiplet. [a]In toluene. [b]In $CDCl_3$. [c]Overlapping signals; coupling $J = 7$ Hz (Et), 6 Hz (Pr^i).

Table 3 Crystallographic data for **2**

chemical formula	$Zr_3PbO_{15}C_{34}H_{76}$
M_w	1205.8
crystal system	monoclinic
space group	$P2_1/n$
Z	4
a/Å	10.618(2)
b/Å	25.157(11)
c/Å	18.611(5)
β/degrees	90.35(2)
V/Å^3	4971(3)
$F(000)$	2408
ρ_{calc}/g cm^{-3}	1.61
μ(Mo-Kα)/cm^{-1}	10
diffractometer	CAD4
monochromator	graphite
radiation	Mo-Kα (0.71070)
scan type	ω–2θ
scan range θ/degrees	$1.2+0.34 \tan \theta$
2θ range/degrees	4–39
reflection collected	4288
reflections used [$I>3\sigma(I)$]	3567
R	0.060
R_w[a]	0.072
weighting scheme	unit weights
rms (shift/e.s.d.) (last ref.)	0.39
least-squares parameters	474

[a] $R_w = [\sum_i w_i (F_o - F_c)^2 / \sum_i w_i F_o^2]^{1/2}$.

parameters, and bond lengths and angles have been deposited at the Cambridge Crystallographic Data Centre (CCDC). See Information for Authors, *J. Mater. Chem.*, 1997, Issue 1. Any request to the CCDC for this material should quote the full literature citation and the reference number 1145/31.

Results and Discussion

Synthesis and characterization of heterometallic alkoxides

The reactions between titanium alkoxides $Ti(OR)_4$ (R = Et, Pr^i), zirconium isopropoxide $[Zr(OPr^i)_4(HOPr^i)]_2$ and various precursors of lead oxide, alkoxides $[Pb(OPr^i)_2]_\infty$, oxoalkoxides $Pb_4O(OR)_6$ (R = Et, Pr^i) and anhydrous acetate $[Pb(OAc)_2]_\infty$ have been investigated. The solvents (hydrocarbons or alcohols) were chosen in order to avoid uncontrolled side reactions such as alcohol exchange reactions and the use of alcohols was thus restricted to the parent alcohol. For similar reasons (absence of redistribution reactions), reactions between metal alkoxides were limited to derivatives having the same OR group. The various compounds were isolated as air-sensitive, colourless crystals. They were characterized by elemental analysis, FTIR and multinuclear NMR (^1H, ^{13}C and ^{207}Pb). Their molecular structures were established by single-crystal X-ray diffraction for $Pb_2Ti_2O(OAc)_2(OPr^i)_8$ **1** and for $PbZr_3O(OAc)_2(OPr^i)_{10}$ **2**.

The insoluble, anhydrous acetate $Pb(OAc)_2$ reacts rapidly at room temperature in non-polar solvents (hexane, toluene) with both titanium and zirconium isopropoxides, as well as titanium ethoxide, giving $Pb_2Ti_2O(OAc)_2(OPr^i)_8$ **1**, $PbZr_3O(OAc)_2(OPr^i)_{10}$ **2** and $[PbTi_2O(OAc)(OEt)_7]_2$ respectively, independent of the stoichiometry between the reactants. The progress of the reaction can be visualized by the complete dissolution of the lead acetate added to the metal alkoxide solution if the appropriate stoichiometry is used. Scheme 1 summarizes the various synthetic routes.

By contrast with the other mixed-metal acetoalkoxides,[23] $Pb_2Ti_2O(OAc)_2(OPr^i)_8$ **1** is only obtained in moderate yield (40%) and an excess of titanium isopropoxide is needed for the reaction with lead acetate in hydrocarbons. This is due to the formation of a titanium byproduct, probably an oxoacetatoalkoxide derivative as evidenced by a $\nu(CO_2)$ absorption band at 1546 cm^{-1}. If the reaction is performed in isopropyl alcohol **1** is obtained selectively and quantitatively. The dimeric zirconium isopropoxide, $[Zr(OPr^i)_4(Pr^iOH)]_2$, was less reactive than the monomeric titanium isopropoxide and a zirconium-rich species, $PbZr_3O(OAc)_2(OPr^i)_{10}$ **2**, was isolated. At first glance, the reactions between group 4 metal alkoxides and $Pb(OAc)_2$ appear dependent on the addition order of the reactants: higher amounts of metal alkoxide are generally necessary for dissolution of $Pb(OAc)_2$ when it is added to a suspension of the lead derivative. However, this observation seems to mainly illustrate differences in kinetics; no other lead species could be detected by ^{207}Pb NMR in such solutions. One can also note the influence of the alkoxide group: derivatives having a different stoichiometry, namely PbM_2 (M = Ti, Zr), were obtained by reacting $Pb(OAc)_2$ with titanium or zirconium ethoxides. $[PbTi_2O(OAc)(OEt)_7]_2$ was obtained independently by other groups[1,14,15] and structurally characterized during the progress of our work. We could also obtain the latter compound quantitatively by adding acetic acid (2 equivalents) to $[PbTi_2O(OEt)_8]_m$ (see below).

Lewis-acid–base reactions between metal alkoxides are one of the most widely investigated routes to mixed-metal oxide precursors.[1,23,24] As we have recently reported, depolymerization of the insoluble lead isopropoxide can be achieved by $Ti(OPr^i)_4$ but requires refluxing in toluene.[13a] The compound isolated, $Pb_2Ti_2O(OPr^i)_{10}$ **3**, has a Pb : Ti stoichiometry attractive for use as a precursor to $PbTiO_3$. The same approach using $[Zr(OPr^i)_4(HOPr^i)]_2$ and $[Pb(OPr^i)_2]_\infty$ did not form Pb–Zr species of 1 : 1 stoichiometry[13b] but species of 4 : 2 and 2 : 4 stoichiometries which do not conproportionate to 1 : 1 species.[26] A variety of alkoxides and oxoalkoxides are known for lead.[18,25] We have used these compounds as alternative sources of lead oxide. **3** can also be obtained by treating $Ti(OPr^i)_4$ with a lead oxoisopropoxide, $Pb_4O(OPr^i)_6$; this reaction proceeds at room temperature since generation of the oxo ligand is no longer required. The reactions between the ethoxide analogues, $Pb_4O(OEt)_6$ and $[Ti(OEt)_4]_m$, are more complex. Mixed-metal species having a different stoichiometry, namely $PbTi_2$, were isolated. Furthermore, compounds having different spectroscopic characteristics (FTIR, ^1H, ^{13}C and ^{207}Pb NMR) were obtained depending on the solvent, ethanol or toluene, and on the order of addition of the reactants. A compound of formula $[PbTi_2O(OEt)_8]_m$ **4** was for instance obtained by adding $Pb_4O(OEt)_6$ to $[Ti(OEt)_4]_m$ in toluene. A different $PbTi_2$ species was isolated by addition of $[Ti(OEt)_4]_m$ to a suspension of $Pb_4O(OEt)_6$. The complexity of the Pb–Ti–OEt system is also illustrated by the numerous ^{207}Pb NMR signals observed upon varying the Pb : Ti molar ratio. These observations are reminiscent of the behaviour of the Ba–Ti–OEt system for which compounds of different stoichiometries, nuclearities and/or number of oxo ligands, could be isolated depending on the experimental conditions.[27] The Pb–Ti–OEt system was not extensively studied due to the lack of isolation of a Pb–Ti species of 1 : 1 stoichiometry and of crystals suitable for X-ray diffraction studies, thus precluding unequivocal structural characterization. One can also observe that, whereas the reaction between $Pb_4O(OEt)_6$ and $Nb(OEt)_5$ proceeds by self-assembly of $Pb_4O(OEt)_6$ giving $Pb_6O_4(OEt)_4$ which acts as a polydentate ligand toward $Nb(OEt)_5$ *via* its peripheral oxo sites,[28] the $Pb_4O(OEt)_6$ aggregate is disrupted during its reaction with titanium ethoxide. Similar observations were reported recently for the reaction between $Pb_4O(OBu^t)_6$ and $Zr(OBu^t)_4$.[29]

The FTIR spectra of the mixed-metal acetoalkoxides are characterized by the symmetrical and asymmetrical stretching of the CO_2 moiety. The differences $\Delta\nu = \nu_{as}(CO_2) - \nu_s(CO_2)$ are in the range 122–196 cm^{-1} and thus suggest that the acetate ligands are either bridging or chelating.[30] Another general feature is the shift to higher frequencies for the CO_2 stretching vibrations of the mixed-metal acetoalkoxides with respect to lead acetate. Similar observations have been made for mixed-metal acetoalkoxides based on other metals.[31] The M—OR

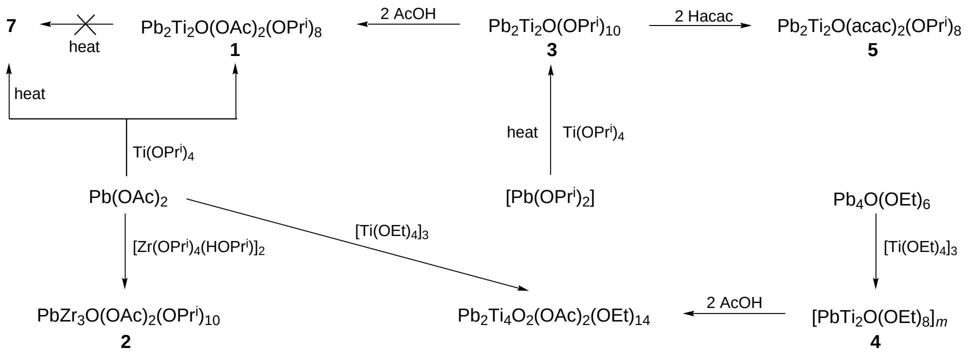

Scheme 1 Synthetic routes to the various Pb–M derivatives (all reactions in toluene at room temperature unless stated otherwise)

stretching vibrations are observed as usual between 600 and 300 cm^{-1} as summarized in Table 1.

Molecular structures of $Pb_2Ti_2O(OAc)_2(OPr^i)_8$ 1 and of $PbZr_3O(OAc)_2(OPr^i)_{10}$ 2 in the solid state and in solution

The existence of heterometallic oxo aggregates has been definitely established by the single-crystal X-ray structure determinations of $Pb_2Ti_2(\mu_4\text{-}O)(\mu\text{-}OAc)_2(OPr^i)_8$ **1** (Fig. 1) and of $PbZr_3O(\mu\text{-}OAc)_2(\mu\text{-}OPr^i)_5(OPr^i)_5$ **2** (Fig. 2). The aggregates are tetranuclear with the metal framework built up around a μ_4-oxo ligand and forming a distorted tetrahedron. The transition metals are six-coordinate with a distorted octahedral stereochemistry. Atomic coordinates and selected bond lengths and angles of **2** are collected in Tables 4 and 5. The mixed-metal acetatoalkoxides **1** and **2** differ essentially by the stoichiometry between the metals, by the orientation of the acetate ligands and by the stereochemistry of the lead centres. For compound **2**, the oxo ligand is the only one connecting atoms Zr(2) and Zr(3) and the corresponding distance between the metals opens up to 4.10 Å by comparison to Zr(1)···Zr(2,3) [3.43 Å (av.)].

The distortion around the zirconium centres of **2** is illustrated by the large variation in the angles from 72.7(4) to 178.4(5)°. The lead atom is five-coordinate with a distorted tetragonal stereochemistry and thus a stereochemically active lone pair.

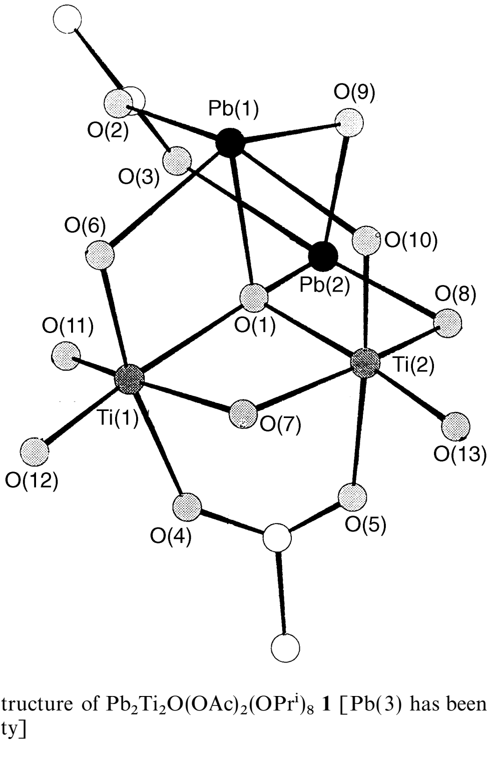

Fig. 1 Structure of $Pb_2Ti_2O(OAc)_2(OPr^i)_8$ **1** [Pb(3) has been omitted for clarity]

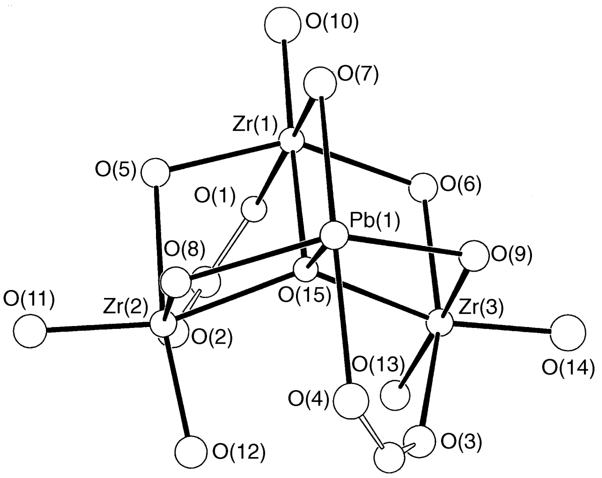

Fig. 2 The $PbZr_3(\mu_4\text{-}O)(\mu\text{-}OAc)_2(\mu_3\text{-}POr^i)_2(\mu\text{-}OPr^i)_4(OPr^i)_4$ **2** molecule showing the crystallographic numbering

The salient feature of the oxo ligand is its 'concave' surrounding, the angle Zr(2)—O(15)—Zr(3) being 134.3(5)°. The Zr—O distances vary from 1.92(1) to 2.26(1) Å and follow the pattern $Zr-OR_t < Zr-\mu\text{-}OR \approx Zr-\mu\text{-}OAc < Zr-\mu_4\text{-}O$, as observed for other heteroleptic zirconium derivatives.[32] The Pb—O bond distances are as expected longer, varying from 2.31(1) to 2.68(1) Å. The Zr—O—C angles associated with terminal OR groups are quite large [from 150.9° to 164(2)°] as usually observed for early transition metals. **2** can be regarded as an adduct between $Pb(OAc)_2$ and $Zr_3O(OPr^i)_{10}$, a moiety which was observed in the mass spectra as a result of the desolvation of $[Zr(OPr^i)_4(Pr^iOH)]_2$.[33] A structural unit, similar to $PbZr_3O(OAc)_2(OPr^i)_{10}$ is found in $Gd_2Zr_6(\mu_4\text{-}O)_2(\mu\text{-}OAc)_2(OPr^i)_{20}$ which results from the assembly *via* bridging acetate ligands of two $GdZr_3O(OAc)_2(OPr^i)_{10}$ moieties.[34]

The structure of $Pb_2Ti_2O(OAc)_2(OPr^i)_8$ **1** is shown in Fig. 1 but no suitable refinement model could be found for all atoms, probably as a result of a disordered lead atom Pb(2). The structural formula $Pb_2Ti_2(\mu_4\text{-}O)(\mu\text{-}OAc)_2(\mu\text{-}OPr^i)_5(OPr^i)_5$ is supported by analytical and spectroscopic data and the tetranuclear core is reasonable in view of the related Pb–M systems. However, bond distances and angles are only deposited as supplementary material. The striking feature is the presence of two types of stereochemistry for the lead centres: Pb(1) is five-coordinate and has a severely distorted tetragonal stereochemistry as observed for the lead centres in **1** and **3**,[13a] while Pb(2) is only four-coordinate, with O—Pb—O angles ranging from 66.2 to 159.6° [for O(3)—Pb—O(8)]. By comparison with $PbZr_3(\mu_4\text{-}O)(OAc)_2(OPr^i)_{10}$ and $Pb_2Ti_2(\mu_4\text{-}O)(OPr^i)_{10}$, the surrounding of the μ_4-oxo ligand is more symmetrical with a Ti(1)—O(1)—Pb(2) angle of 101.8°. Both acetate ligands are bridging, they assemble identical metals while they bridge lead

Table 4 Fractional parameters for **2**

atom	*x*/*a*	*y*/*b*	*z*/*c*	*U*(equiv.)/Å^2
Pb(1)	0.47277(8)	0.07863(3)	0.25025(5)	0.0284
Zr(1)	0.8007(2)	0.04496(8)	0.2329(1)	0.0240
Zr(2)	0.7124(2)	0.12923(8)	0.3673(1)	0.0258
Zr(3)	0.6860(2)	0.15735(8)	0.1507(1)	0.0251
O(1)	0.966(1)	0.0931(5)	0.2502(6)	0.0056
O(2)	0.903(1)	0.1497(6)	0.3370(7)	0.0325
O(3)	0.555(1)	0.2132(5)	0.1968(8)	0.0402
O(4)	0.415(1)	0.1718(6)	0.2636(8)	0.0391
O(5)	0.796(1)	0.0482(5)	0.3455(7)	0.0270
O(6)	0.798(1)	0.0862(5)	0.1342(7)	0.0304
O(7)	0.640(1)	0.0029(5)	0.2234(7)	0.0359
O(8)	0.536(1)	0.0928(5)	0.3746(7)	0.0231
O(9)	0.521(1)	0.1101(5)	0.1358(7)	0.0288
O(10)	0.911(1)	−0.0137(5)	0.2132(9)	0.0392
O(11)	0.754(1)	0.1217(6)	0.4688(7)	0.0307
O(12)	0.667(1)	0.2030(5)	0.3663(8)	0.0366
O(13)	0.820(1)	0.2044(5)	0.1789(7)	0.0263
O(14)	0.674(1)	0.1770(6)	0.0510(7)	0.0396
O(15)	0.6766(9)	0.1107(4)	0.2518(5)	0.004(2)
C(1)	0.984(2)	0.131(1)	0.295(1)	0.0189
C(2)	1.118(2)	0.157(1)	0.300(1)	0.0446
C(3)	0.455(2)	0.2109(9)	0.234(1)	0.0336
C(4)	0.382(2)	0.263(1)	0.239(2)	0.0467
C(5)	0.849(2)	0.0144(9)	0.400(1)	0.0387
C(6)	0.990(2)	0.019(1)	0.401(1)	0.0492
C(7)	0.804(3)	−0.041(1)	0.387(1)	0.0609
C(8)	0.871(2)	0.070(1)	0.077(1)	0.0811
C(9)	0.981(3)	0.105(2)	0.059(2)	0.1036
C(10)	0.797(3)	0.045(2)	0.016(1)	0.1104
C(11)	0.607(3)	−0.052(1)	0.213(2)	0.0596
C(12)	0.607(4)	−0.065(1)	0.136(2)	0.0917
C(13)	0.491(3)	−0.064(1)	0.252(2)	0.0798
C(14)	0.462(2)	0.084(1)	0.434(1)	0.0518
C(15)	0.403(3)	0.131(1)	0.462(2)	0.0690
C(16)	0.384(4)	0.039(1)	0.424(2)	0.1041
C(17)	0.432(2)	0.110(1)	0.078(1)	0.0472
C(18)	0.334(3)	0.154(1)	0.087(2)	0.0740
C(19)	0.377(3)	0.059(1)	0.070(2)	0.0961
C(20)	1.002(2)	−0.047(1)	0.182(2)	0.0942
C(21)	1.134(2)	−0.030(1)	0.203(2)	0.0960
C(22)	0.976(3)	−0.104(1)	0.200(3)	0.1496
C(23)	0.786(2)	0.143(1)	0.534(1)	0.0947
C(24)	0.717(3)	0.118(1)	0.595(1)	0.0887
C(25)	0.927(3)	0.143(2)	0.545(1)	0.0933
C(26)	0.665(2)	0.2576(9)	0.375(1)	0.0458
C(27)	0.793(3)	0.278(1)	0.397(2)	0.0693
C(28)	0.562(3)	0.272(1)	0.428(2)	0.0690
C(29)	0.893(2)	0.249(1)	0.192(1)	0.0524
C(36)	0.816(3)	0.299(1)	0.183(2)	0.0677
C(31)	1.008(3)	0.249(1)	0.147(2)	0.0894
C(32)	0.706(3)	0.204(1)	−0.009(1)	0.1419
C(33)	0.651(5)	0.260(1)	−0.010(2)	0.1347
C(34)	0.674(4)	0.173(2)	−0.077(1)	0.1023

Table 5 Selected bond lengths (Å) and angles (°) for **2**

Pb(1)–O(4)	2.44(1)	Zr(1)–O(1)	2.15(1)
Pb(1)–O(9)	2.33(1)	Zr(1)–O(6)	2.11(1)
Pb(1)–O(8)	2.43(1)	Zr(1)–O(10)	1.92(1)
Pb(1)–O(15)	2.310(9)	Zr(1)–O(5)	2.10(1)
Pb(1)–O(7)	2.66(1)	Zr(1)–O(7)	2.02(1)
Zr(2)–O(2)	2.17(1)	Zr(1)–O(15)	2.15(1)
Zr(2)–O(8)	2.09(1)	Zr(3)–O(3)	2.16(1)
Zr(2)–O(12)	1.92(1)	Zr(3)–O(9)	2.14(1)
Zr(2)–O(5)	2.26(1)	Zr(3)–O(14)	1.92(1)
Zr(2)–O(11)	1.95(1)	Zr(3)–O(6)	2.17(1)
Zr(2)–O(15)	2.23(1)	Zr(3)–O(13)	1.92(1)
Pb(1)–Zr(1)	3.58(2)	Zr(3)–O(15)	2.22(1)
Pb(1)–Zr(2)	3.58(2)	Zr(1)···Zr(2)	3.414(3)
Pb(1)–Zr(3)	3.54(2)	Zr(1)···Zr(3)	3.434(3)
O(8)–Pb(1)–O(4)	80.2(5)	Zr(2)···Zr(3)	4.10(3)
O(9)–Pb(1)–O(8)	139.4(4)	O(9)–Pb(1)–O(4)	79.9(5)
O(15)–Pb(1)–O(8)	71.5(4)	O(15)–Pb(1)–O(4)	84.3(4)
O(15)–Pb(1)–O(7)	68.07(4)	O(15)–Pb(1)–O(9)	71.5(4)
O(7)–Pb(1)–O(9)	85.32(4)	O(7)–Pb(1)–O(8)	96.09(4)
O(5)–Zr(1)–O(1)	81.6(5)	O(7)–Pb(1)–O(4)	151.57(4)
O(6)–Zr(1)–O(1)	82.1(5)	O(10)–Zr(1)–O(6)	102.5(6)
O(6)–Zr(1)–O(5)	148.3(5)	O(10)–Zr(1)–O(7)	95.7(6)
O(7)–Zr(1)–O(1)	175.4(5)	O(15)–Zr(1)–O(1)	92.4(4)
O(7)–Zr(1)–O(5)	94.8(5)	O(15)–Zr(1)–O(5)	77.8(4)
O(7)–Zr(1)–O(6)	99.9(5)	O(15)–Zr(1)–O(6)	76.0(4)
O(10)–Zr(1)–O(1)	87.8(5)	O(15)–Zr(1)–O(7)	84.1(5)
O(10)–Zr(1)–O(5)	103.8(6)	O(15)–Zr(1)–O(10)	178.4(5)
O(5)–Zr(2)–O(2)	78.4(5)	O(6)–Zr(3)–O(3)	161.3(5)
O(8)–Zr(2)–O(2)	163.7(5)	O(9)–Zr(3)–O(3)	83.4(5)
O(8)–Zr(2)–O(5)	88.2(5)	O(9)–Zr(3)–O(6)	88.4(5)
O(11)–Zr(2)–O(2)	93.8(5)	O(13)–Zr(3)–O(3)	88.0(5)
O(11)–Zr(2)–O(5)	89.9(5)	O(13)–Zr(3)–O(6)	98.3(5)
O(11)–Zr(2)–O(8)	95.4(6)	O(13)–Zr(3)–O(9)	169.9(6)
O(12)–Zr(2)–O(2)	90.0(6)	O(14)–Zr(3)–O(3)	100.2(6)
O(12)–Zr(2)–O(5)	165.8(5)	O(14)–Zr(3)–O(6)	96.2(6)
O(12)–Zr(2)–O(8)	101.7(5)	O(14)–Zr(3)–O(9)	88.2(6)
O(12)–Zr(2)–O(11)	99.2(6)	O(14)–Zr(3)–O(13)	98.5(6)
O(15)–Zr(2)–O(2)	87.3(4)	O(15)–Zr(3)–O(3)	88.6(5)
O(15)–Zr(2)–O(5)	72.7(4)	O(15)–Zr(3)–O(6)	73.2(4)
O(15)–Zr(2)–O(8)	79.9(4)	O(15)–Zr(3)–O(9)	77.0(4)
O(15)–Zr(2)–O(11)	162.0(5)	O(15)–Zr(3)–O(13)	97.6(5)
O(15)–Zr(2)–O(12)	98.7(5)	O(15)–Zr(3)–O(14)	161.8(5)

and zirconium in $PbZr_3O(OAc)_2(OPr^i)_{10}$. The Pb—O distances range from 2.09(3) to 2.79(3) Å, the Pb—μ_4-O distances are shorter than the Pb—μ-OR ones, while the Pb—OAc bond distances have intermediate values. The Ti—O bond distances spread over the range 1.77(3)–2.12(2) Å and follow the order Ti—OR$_t$ < Ti—μ-OR ≈ Ti—μ_4-O < Ti—OAc as observed for other titanium acetatoalkoxides.[35]

Both structures are related to that of $Pb_2Ti_2O(OPr^i)_{10}$.[13a] However, in the absence of bidentate OAc ligands for **3**, two OR are triply bridging capping two Pb_2Ti faces of the tetrahedron as a means to ensure hexacoordination of titanium. Although the tetrahedron is fairly regular, the coordination geometry of the μ_4-oxo ligand is also distorted. Assembly of the various metals around a μ_4-oxo ligand has also been observed for the other reported Pb–M (M = Ti, Zr) acetatoalkoxide derivatives such as $[PbTi_2(\mu_4\text{-}O)(OAc)(OEt)_7]_2$[14] and $[PbZr_2(\mu_4\text{-}O)(OAc)_2(OEt)_6]_2$.[16] Although these structures are based on M_2M_4 dimers, they can be alternatively seen as derived from $PbM_3(\mu_4\text{-}O)$ tetrahedra fused along a hypothetical Pb—Pb edge in the case of the titanium mixed-metal compound and along a M—M edge for the zirconium derivative.

The various aggregates are soluble in non-polar solvents such as toluene and no dissociation is observed as shown by NMR (^{1}H, ^{13}C, ^{207}Pb). The presence of only one signal in the ^{207}Pb NMR spectrum of **1** suggests dynamic behaviour.† ^{1}H NMR spectra at variable temperature and dilution are consistent with the presence in solution of two fluxional molecular species mainly, **1A** and **1B**, in dynamic exchange. For the concentration range 0.3–0.03 M, these two species are present in a proportion close to 2 : 1 as indicated by the presence in the low-temperature spectra of three types of magnetically non-equivalent acetate ligands (integration ratio 1 : 1 : 1). In the region of the methine groups, the broad multiplet observed at room temperature corresponds to mainly four septets at δ 4.47, 4.71, 4.89 and 5.15, respectively. They have been attributed to terminal and doubly bridging OR groups of types Pb—OR—Pb, Ti—OR—Ti and Pb—OR—Ti of species **1A** and **1B**. Conversion between isomer **1A**, having the solid-state structure, and isomer **1B** (Scheme 2) is in agreement with the spectroscopic data. Species **1A** displays two types of non-equivalent acetate ligands. Isomer **1B** displays only one type of bridging acetate ligand and one type of surrounding for the lead centres. The latter isomer derives from species **1A**, which is preponderant in solution, by transformation of one bridging OR ligand [on Ti(1)] into a terminal one and modification of the coordination modes of the acetate ligands,

---

† Two chemical shifts were observed at 300 MHz for **1** (ref. 15).

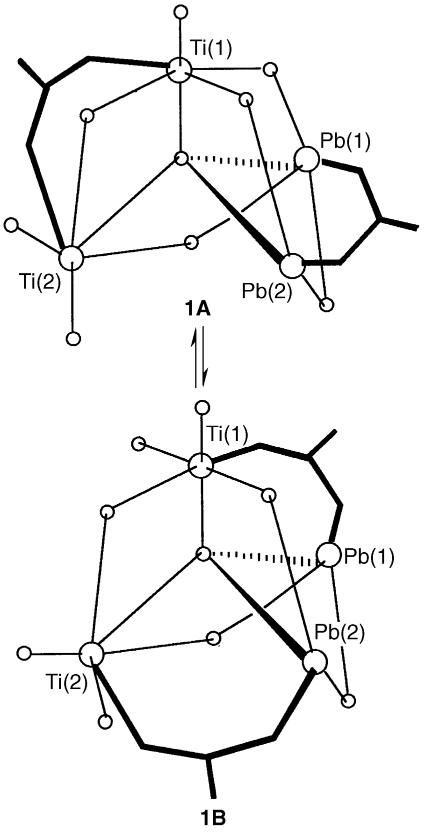

Scheme 2 Interconversion of the $Pb_2Ti_2O(OAc)_2(OPr^i)_8$ species **1A** and **1B** in solution

each one assembling the two different metals, lead and titanium, as observed for the Pb–Zr species. The open site at one of the lead centres of **1** favours the migration of the OAc ligand. $Pb_2Ti_4O_2(OAc)_2(OEt)_{14}$ is also fluxional but its behaviour has not been fully investigated.

By contrast to **1** and **3**, $PbZr_3O(OAc)_2(OPr^i)_{10}$ **2** and $[PbTi_2O(OEt)_8]_m$ **4** are non-fluxional. The ^1H NMR spectrum of **2** displays two signals for the acetate ligands in a 1:1 integration ratio while the signals of the methine groups are spread over the range δ 4.25–5.15 and five types of magnetically non-equivalent groups are observed. These data are consistent with the solid-state structure. All species are more stable than $[PbZr_2(\mu_4\text{-}O)(OAc)_2(OEt)_6]_2$ which has been reported to exist in solutions as several molecular species as illustrated by the observation of three ^{207}Pb NMR resonances.[16] The ^1H NMR spectra of **4** indicate three types of magnetically different CH_2 groups in a 2:4:2 integration ratio at low temperature ($-40\,°C$). A unique signal is observed in the ^{207}Pb NMR spectrum at δ 2560. In the absence of X-ray data, several structures might account for the spectroscopic data. Structure **C**, resulting from the junction of two Pb_2Ti_2 units along a Pb—Pb edge, is consistent with the spectroscopic data. The carboxylate derivative $Pb_2Ti_4O_2(OAc)_2(OEt)_{14}$, which could be obtained quantitatively by addition of acetic acid to **4**, has a structure related to **C**, one bridging alkoxide of type Ti—OR—Ti being substituted by an acetate ligand.[15] The selectivity of the conversion of **4** into the acetate derivative, especially the retention of the stoichiometry between the metals, is also in favour of structure **C**.

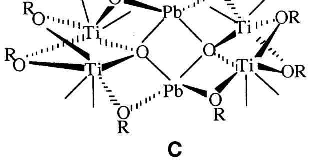

C

Reactivity

The presence of the oxo ligand allows the transition metals to achieve their most common coordination number, namely six. The various compounds thus already possess in the precursors the coordination numbers required for Zr and Ti in the perovskite structure. The oxo ligand might derive from the alkoxide ligands by elimination of dialkyl ether, from the acetate by formation of an ester, by hydrolysis during the work-up or by residual water from lead acetate.‡ The oxo derivatives are obtained in high and reproducible yield (thus excluding accidental hydrolysis) and ^{207}Pb NMR monitoring shows no other Pb–M intermediates. No presence of ester could be detected by FTIR in the various reaction media and the alkoxide ligands are thus the most likely source of the oxo ligand. Isopropyl acetate detected by FTIR [$\nu(CO_2) = 1745\ cm^{-1}$] is however formed if the heterogeneous reaction medium, obtained by mixing $Ti(OPr^i)_4$ and $Pb(OAc)_2$ in toluene, is heated, prior to the dissolution of the acetate and thus to the formation of **1**. The elimination of the ester corresponds to the formation of an insoluble metal acetato-alkoxide species [$\nu(CO_2) = 1559\ cm^{-1}$]. The presence of a broad absorption band around 798 cm^{-1} in its FTIR spectrum suggests the formation of an extended M—O—M network and thus of polymeric species. However, compound **1**, once formed, is stable toward thermal condensation: no evolution is observed after 12 h of reflux in Pr^iOH.

The quite easy depolymerization of $[Pb(OPr^i)_2]_\infty$ by metal alkoxides is due to the facile formation of lead oxoalkoxides.[18] Compound **3** can formally be considered as $Pb_4O(OPr^i)_6$ in which two lead sites have been substituted by $Ti(OPr^i)_2$ moieties. Attempts to build up mixed-metal species containing a chloride as a functional ligand (as intermediates to terhetero-metallic species) by using a chloroalkoxide $Ti(OPr^i)_3Cl$ as a starting titanium material and $Pb_4O(OPr^i)_6$ in toluene at room temperature were prevented by the precipitation of $PbCl_2$.

The Pb–Ti acetatoalkoxide **1** could also be obtained by the addition of acetic acid (2 equivalents) to $Pb_2Ti_2O(OPr^i)_{10}$ in hexane. The modification of **3** by acetylacetone, which is another reactant commonly used in the sol–gel process[36] in order to control the hydrolysis rates and/or avoid precipitation, afforded $Pb_2Ti_2O(acac)_2(OPr^i)_8$ **5**, when small amounts (2 equivalents) of reactant were used (Scheme 1).[13a] By contrast to the OAc ligands, the acac ligands seem to behave as terminal-chelating ligands located on the titanium centres according to the FTIR and ^1H NMR data, which are close to those reported for $Ti(OPr^i)_2(acac)_2$. The analogy in ^{207}Pb NMR chemical shifts between **3** (δ 3870) and **5** (δ 3883) suggests also that the surrounding of the lead atoms is only slightly modified by the transformation of **3** into **5**. Chemical modification reactions of mixed-metal alkoxides are generally difficult to control and change of the stoichiometry between the metals, the main-group element being extruded as an insoluble derivative, is easily observed.[23] The structural similarity between compounds **1**, **3** and **5** allows conservation of the Pb:Ti stoichiometry by substitution of two OR by OAc or acac ligands, titanium remaining hexacoordinated. Larger amounts of acetic acid or acetylacetone lead to the precipitation of $Pb(OAc)_2$ or the formation of $Ti(acac)_2(OPr^i)_2$ respectively, and thus to segregation of the mixed-metal species **3**. Acetylacetone has been considered to improve the quality of $PbTiO_3$ coatings during thermal annealing when added to $Pb(OAc)_2$–$Ti(OR)_4$ solutions. Its influence on **1** was therefore considered. When **1** is reacted with one equivalent of Hacac in toluene at room temperature, precipitation of $Pb(OAc)_2$ is

---

‡ Among the various methods of obtaining anhydrous acetates, dehydration of $Pb(OAc)_2 \cdot 3H_2O$ with acetic anhydride gave the best results in terms of residual water (<0.2%) and the same lead acetate was used to obtain quantitatively non-oxo mixed-metal acetatoalkoxides.

observed, probably facilitated by the fluxionality of **1** and the stability of $Ti(OPr^i)_2(acac)_2$.

As a general feature, the lead chemical shifts of the mixed-metal species are observed at higher field than those of the homometallic lead alkoxides or oxoalkoxides, in which the lead atoms display lower coordination numbers. Lead NMR can thus be used as a tool for the indication of the formation of mixed-metal Pb–M species (M = Ti, Nb, Bi) and thus of some homogeneity at the molecular level.

Microhydrolysis experiments of $Pb_2Ti_2O(OAc)_2(OPr^i)_8$ **1** have been achieved. The concept of a 'molecular building block' approach relies on a knowledge of the nature of the initial precursor as well as on its transformation. A soluble, microcrystalline species **6a** could be isolated if microhydrolysis experiments were performed in toluene with a hydrolysis ratio h as low as 0.5 or 1 (hydrolysis ratio h = moles H_2O/moles PbTi precursor). Analytical and spectroscopic data indicate an empirical formula $[Pb_4Ti_4O_6(OAc)_4(OPr^i)_8]_m$ [$\nu_{as}(CO_2) = 1585$, 1543 cm^{-1}]. Further evolution into a new species **6b** is however observed during recrystallisation. Compound **6b**, of formula $[Pb_4Ti_4O_7(OAc)_4(OPr^i)_6]_m$, displays a FTIR spectrum similar to that of **6a** for the absorption bands corresponding to the acetate ligands while the disappearance of the ν(M—OR) band at 490 cm^{-1} supports further condensation. The presence of metal–oxo vibrations is illustrated by quite sharp bands at 834, 802, 748 and 722 cm^{-1}. It is noticeable that **6b** can also be obtained as a minor species by hydrolysis of **1** in THF using larger amounts of water ($h = 2$), together with an insoluble material **7**. The high solubility (even in hexane) of **6a** and **6b** suggests *closo* structures with peripheral organic groups. By contrast, compound **7**, which is the predominant species obtained for $h = 2$, is not soluble in THF. Its FTIR characteristics [$\nu_{as}(CO_2) = 1550$, ν(M—O—M) 800 cm^{-1}] are similar to those of the compound obtained by heating $Ti(OPr^i)_4$ and $Pb(OAc)_2$ immediately after mixing. Proton NMR data of **6a** at various temperatures indicate three types of acetate ligands in a 1 : 1 : 2 ratio and four types of methine groups in a 2 : 2 : 1 : 3 ratio. A structure of type **D** is in agreement with these spectroscopic data. It displays six-coordinated titanium centres and four- and five-coordinated lead, as observed in the non-hydrolysed precursor **1**. The proposed octanuclear structure can be considered as the assembly, *via* doubly bridging oxo ligands resulting from the hydrolysis of terminal OR groups borne by titanium atoms, the most electropositive centres, of two tetranuclear dioxo moieties. The tetranuclear subunits can be considered as resulting from hydrolysis of species **1a** and **1b**, the site of attack being a doubly bridging OR group, as supported by literature data on other mixed-metal species.[37] The overall observations suggest that if small structural reorganisation is likely in the very first steps of the hydrolysis, more drastic transformations are necessary for the passage to the material. Unfortunately, the poor stability in solution of **6a** and **6b** precluded obtaining crystals suitable for X-ray studies.

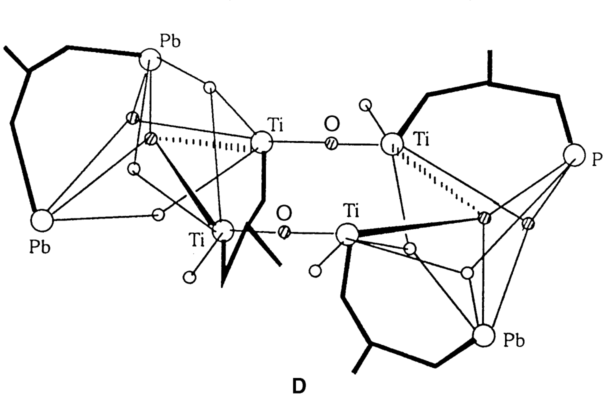

D

Hydrolysis–polycondensation

The potential of these novel mixed-metal Pb–M species (M = Ti, Zr) as precursors to lead-based materials was estimated, especially for the compounds having stoichiometries with materials formulation and which may thus act as single-source precursors to $PbTiO_3$, namely **1**, **3** and **5**. Hydrolyses were achieved at room temperature. The amorphous powders were characterized by FTIR, thermogravimetric analysis (TG), differential thermal analysis (DTA) and X-ray diffraction (XRD) at variable temperatures after thermal treatment.

Although the metal ratios of $PbZr_3O(OAc)_2(OPr^i)_{10}$ **2** and of $[PbTi_2O(OEt)_8]_m$ **4** did not match those of lead-based ferroelectrics, such compounds might find use as dopants or give access to nanocomposites. Their behaviour as precursors in hydrolysis–polycondensation reactions was thus also investigated. $[PbTi_2O(OEt)_8]_m$ gives $PbTi_3O_7$ and red lead oxide at 650 °C. The same material is obtained from $[PbTi_2O(OAc)(OEt)_7]_2$ at 600 °C. $PbZr_3O(OAc)_2(OPr^i)_{10}$ is converted into $PbZrO_3$ and cubic zirconia at 800 °C, the latter being already obtained at 600 °C, together with an amorphous matrix. The composition of these multiphased materials is thus largely dependent on the temperature of the thermal treatment.

Hydrolysis–polycondensation reactions of **1**, **3** and **5**, were achieved in isopropyl alcohol at room temperature at concentrations of 0.01 M and with a hydrolysis ratio $h = 100$. FTIR spectra of the powders resulting from $Pb_2Ti_2O(OAc)_2(OPr^i)_8$ **1** and $Pb_2Ti_2O(acac)_2(OPr^i)_8$ **5** show absorption bands characteristic of acetate [$\nu_{as}(CO_2) = 1544$, $\nu_s(CO_2) = 1412$ cm^{-1}] and of acetylacetonate ligands [ν(C—O), ν(C=C) = 1576, 1506, 1460, 1385 cm^{-1}], respectively, as well as hydroxy residues [$\nu(OH) = 3400$ cm^{-1}]. These observations account for the differing degrees of hydrolysis of **5** and **1**. For the latter, some of the acetate ligands are removed as isopropyl acetate [$\nu_{as}(CO_2) = 1745$ cm^{-1}] and thus are released in the filtrate.

The hydrolysis–polycondensation process leads to precipitates for compounds **1** and **3**, while **5** gives turbid sols. These observations are supported by measurement of the particle sizes (9800 nm for **1** and 4120 nm for **3** but only 100 and 340 nm for **5**). While the particles are monodisperse for **1** and **3**, two distributions were observed for **5** (79 and 21%, respectively). These observations might be explained by the tendency of acetates to act as assembling ligands whereas acetylacetonates are more prone to act as polymerization lockers and thus favour the formation of smaller particles.

Thermogravimetric and differential thermal analyses have been performed under nitrogen or air up to 1000 °C. Elimination of organic residues starts at about 100 °C; that of the remaining ligands acetate and acetylacetonate occurs below 400 °C. The smallest weight loss is observed for the powder resulting from the hydrolysis of $Pb_2Ti_2O(OPr^i)_{10}$ **3** (8.5%) by comparison to **1** and **5** (20 and 26% respectively). DTA profiles show broad exothermic peaks corresponding to the combustion of the organics while a sharper exothermic peak suggesting crystallisation is observed towards 500 °C (Fig. 3A). Thermal treatment of the various amorphous powders afforded the crystalline $PbTiO_3$ perovskite but some differences can be noticed depending on the precursors. The powders resulting from the hydrolysis of **1** and **5** lead directly to the perovskite phase at 550 and 500 °C, respectively (Fig. 3B). The powder resulting from $Pb_2Ti_2O(OPr^i)_{10}$ behaves differently: crystallisation starts at 500 °C giving a mixture of perovskite $PbTiO_3$ (25%) and pyrochlore $Pb_2Ti_2O_6$ {% perovskite calculated as [perovskite]/[perovskite + pyrochlore]}. Conversion of pyrochlore into perovskite is complete at 700 °C and pure perovskite is then obtained. It should be noted that the hydrolysis of **1** with smaller amounts of water ($h = 0$–40) in isopropyl alcohol was reported to proceed *via* the formation of some pyrochlore.[38]

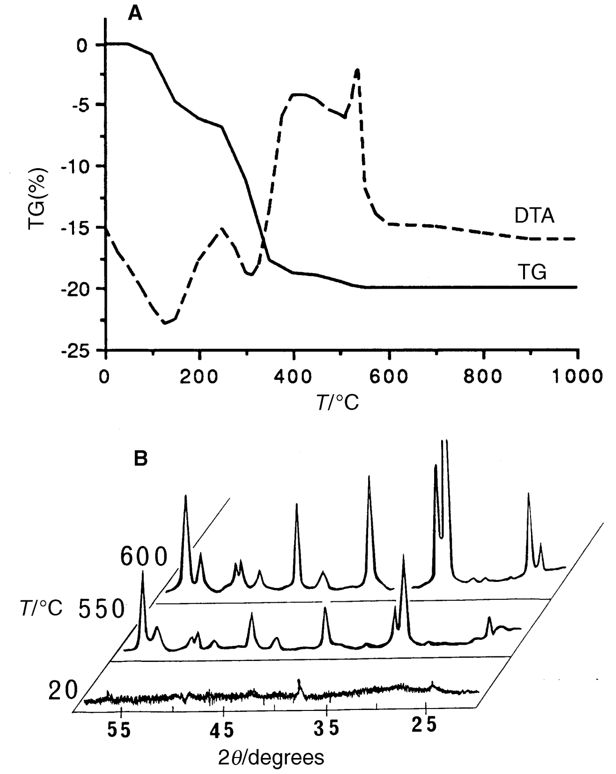

Fig. 3 **A**, TG trace of the powder resulting from hydrolysis of **1** and **B**, X-ray diffraction patterns at various temperatures

Influence of the solvent

Sol–gel processing of $PbTiO_3$ has been widely investigated. Recently the presence of acetone during the hydrolysis step has been reported to lower the temperature of crystallisation of $PbTiO_3$ to 250 °C.[39] This prompted us to investigate the influence of that solvent on the polycondensation of the various Pb–Ti precursors of 1 : 1 stoichiometry.

Acetone reacts immediately at room temperature with **1**, **3** and **5** giving precipitates whose FTIR characteristics [ν(OH) *ca.* 3400 cm^{-1}, residual OAc or acac ligands, broad M—O—M absorption] are similar to those obtained by the preceding hydrolysis–polycondensation reactions indicating that acetone induces non-hydrolytic condensation reactions.[40] However, since these reactions were difficult to control regarding particle size and formation of agglomerates, acetone was used as a co-solvent with isopropyl alcohol for the hydrolysis–polycondensation reactions. Whereas the influence of acetone was not significant regarding the temperature of crystallisation, it was more important for the control of the nature of the crystalline phases and particle size.

Hydrolysis of $Pb_2Ti_2O(OPr^i)_{10}$ in acetone–isopropyl alcohol (50 : 50 v/v) led to an amorphous powder which was converted directly into perovskite upon calcination at 600 °C. The presence of acetone thus avoids the formation of pyrochlore as an intermediate. Another benefit of the presence of acetone is the reduction of the particle size. By using $Pb_2Ti_2O(OAc)_2(OPr^i)_8$ as a precursor, the size of the particles decreases from 9800 nm (pure isopropyl alcohol) to 9450 nm [isopropyl alcohol–acetone (80 : 20 v/v)] and finally 235 nm for isopropyl alcohol–acetone (20 : 80). Comparable observations are seen for **3** and **5**. Hydrolysis of $Pb_2Ti_2O(OPr^i)_{10}$ in isopropyl alcohol–acetone (50 : 50) gives a precipitate composed of particles of diameter 682 nm. For $Pb_2Ti_2O(acac)_2(OPr^i)_8$, a sol stable at least for five weeks, is obtained from isopropyl alcohol–acetone (20 : 80). Measurements of the particle size show that the sol consists of nanoparticles with a diameter of 10 nm. For the composition of 50 : 50, the particles are much larger [1650 nm (66%) and 240 nm (34%)]. These observations suggest that the control of the particle size *via* the use of acetone requires an appropriate choice of the solvent composition. Fig. 4 shows histograms obtained for the particles resulting from the hydrolysis–polycondensation of **1** and **3** in isopropyl alcohol–acetone (20 : 80) and shows the influence of the ancillary ligand OAc *vs.* acac.

The influence of various other factors was estimated for the hydrolysis of **1** in isopropyl alcohol–acetone (20 : 80). Hydrolysis in basic conditions (NH_3, 1 M) resulted in crystallisation already at 500 °C but pyrochlore was present together with perovskite (40%). Hydrolysis at room temperature followed by refluxing over 20 h and calcination under dioxygen in order to favour the elimination of the organic residues did not significantly reduce the temperature of crystallisation.

Conclusion

Different Pb–Ti mixed-metal alkoxides having a stoichiometry matching that of $PbTiO_3$ can be obtained. They are all based on isopropoxides as the alkoxide ligand and while chemical homogeneity can be obtained by using ethoxides, the stoichiometry is no longer that required for $PbTiO_3$. Access to Pb–Zr species of 1 : 1 stoichiometry appears more tedious.[13b,29] Better homogeneity at the molecular level thus exists for the Pb–Ti system than for the Pb–Zr one which in turn leads to lower onset of crystallisation and lower tendency of segregation of the MO_2 phase, although zirconium is also hexacoordinated in all Pb–Zr species except $Pb_2Zr_4(\mu_4\text{-}O)_2(OAc)_4(OEt)_{12}$ structurally characterized so far. The various mixed-metal species are non-volatile, they can thus not be used for classical, thermal MOCVD. However their solubility is compatible with their use in aerosol-assisted CVD techniques (AACVD).[41]

We thank the CNRS (GRECO 93 'Sol-gel inorganiques') for financial support and Dr F. Chaput (Paris) for the powder XRD data.

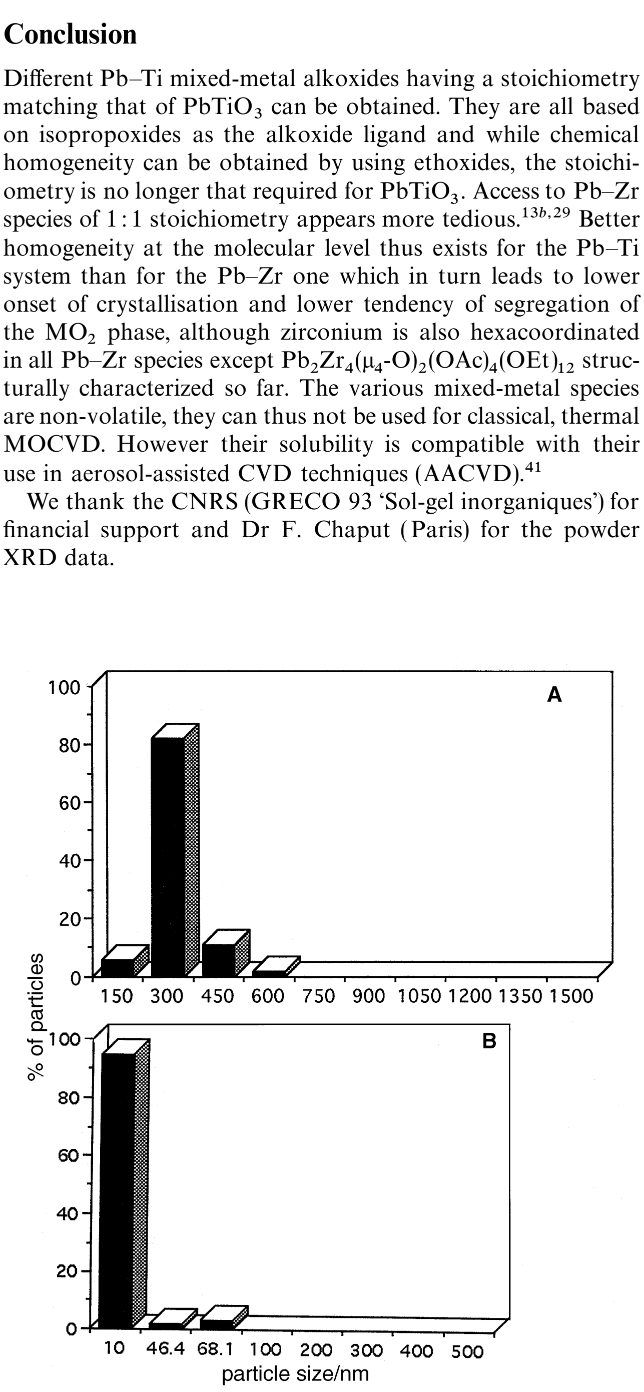

Fig. 4 Histograms showing the size distribution for the particles resulting from the hydrolysis–polycondensation of **1** (**A**) and of **3** (**B**) in isopropyl alcohol–acetone (20 : 80)

References

1. C. D. Chandler, C. Roger and M. J. Hampden-Smith, *Chem. Rev.*, 1993, **93**, 1205.
2. R. A. Assink and R. W. Schwartz, *Chem. Mater.*, 1993, **5**, 511.
3. S. R. Gurkovich and J. B. Blum, *Ultrastructure Processing of Ceramics, Glasses, and Composites*, ed. L. L. Hench and D. R. Ulrich, J. Wiley, New York, 1984, p. 152.
4. K. D. Budd, S. K. Dey and D. A. Payne, *Proc. Br. Ceram. Soc.*, 1985, **36**, 107.
5. C. Chen, D. F. Ryder Jr. and W. A. Spurgeon, *J. Am. Ceram. Soc.*, 1989, **72**, 1495.
6. O. Yamaguchi, A. Narai, T. Komatsu and K. Shimizu, *J. Am. Ceram. Soc.*, 1986, **69**, C256; M. L. Calzada and S. J. Milne, *J. Mater. Sci. Lett.*, 1993, **12**, 1221; N. J. Philipps and S. J. Milne, *J. Mater. Chem.*, 1991, **1**, 893; R. Sirrera, M. L. Calzada and F. Carmona and B. Jimenez, *J. Sol–Gel Sci. Technol.*, 1994, **2**, 545; L. Pardo, L. M. Calzada, S. J. Milne, J. Ricote and J. Jimenez, *Phys. Chem.*, 1995, **56**, 15.
7. N. Tohge, S. Takahashi and T. Minami, *J. Am. Ceram. Soc.*, 1991, **74**, 67; H. Hirashima, E. Onishi and M. Nakagawa, *J. Non-Cryst. Solids*, 1990, **121**, 404.
8. C. D. Chandler, M. J. Hampden-Smith and C. J. Brinker, *Mater. Res. Soc. Symp. Proc.*, Pittsburgh, 1992, vol. 271, p. 89.
9. C. D. Chandler, M. J. Hampden-Smith and E. N. Duesler, *Inorg. Chem.*, 1992, **31**, 4891.
10. C. D. E. Lakeman and D. A. Payne, *J. Am. Chem. Soc.*, 1992, **75**, 3091.
11. S. D. Ramamurthi and D. A. Payne, *Mater. Res. Soc. Symp. Proc.*, 1990, vol. 180, p. 79; S. D. Ramamurthi and D. A. Payne, *J. Am. Ceram. Soc.*, 1990, **73**, 2547.
12. S. S. Sengupta, L. Ma, D. L. Adler and D. A. Payne, *J. Mater. Res.*, 1995, **10**, 1345.
13. (*a*) S. Daniele, R. Papiernik, L. G. Hubert-Pfalzgraf, S. Jagner and M. Hakansson, *Inorg. Chem.*, 1994, **34**, 628; (*b*) M. C. Massiani, Thesis, Nice, 1992.
14. H. K. Chae, D. A. Payne and Z. Xu, *Chem. Mater.*, 1994, **6**, 1583.
15. J. Bates, Q. Zhang, L. Spiccia and B. O. West, *J. Sol–Gel Sci. Technol.*, 1994, **2**, 29.
16. L. Ma and D. A. Payne, *Chem. Mater.*, 1994, **6**, 875.
17. L. G. Hubert-Pfalzgraf, *Better Ceramics Through Chemistry V, Mater. Res. Soc. Symp. Proc.*, Pittsburgh, 1992, vol. 271, p. 15 and references therein.
18. R. Papiernik, L. G. Hubert-Pfalzgraf and M. C. Massiani, *Polyhedron*, 1991, **10**, 1657.
19. B. A. Vaarstra, J. C. Huffman, P. S. Gradeff, L. G. Hubert-Pfalzgraf, J. C. Daran, S. Parraud, K. Yunlu and K. G. Caulton, *Inorg. Chem.*, 1990, **29**, 3126.
20. D. J. Watkin, J. R. Carruthers and P. W. Betteridge, CRYSTALS User Guide, Chemical Crystallography Laboratory, University of Oxford, 1986.
21. *International Tables for X-Ray Crystallography*, Kynoch Press, Birmingham, 1974, vol. IV.
22. N. Walker and D. Stuart, *Acta Crystallogr., Sect. A*, 1983, **39**, 159.
23. L. G. Hubert-Pfalzgraf, *Polyhedron*, 1994, **13**, 1181.
24. K. G. Caulton and L. G. Hubert-Pfalzgraf, *Chem. Rev.*, 1990, **90**, 969.
25. S. C. Goel, M. Y. Chiang and W. E. Buhro, *Inorg. Chem.*, 1990, **29**, 4640.
26. D. J. Teff, J. C. Huffman and K. G. Caulton, *Inorg. Chem.*, 1995, **34**, 2491.
27. A. I. Yanovskii, E. P. Turevsskoya, M. I. Yanovskaya, V. G. Kessler, N. Ya Turova, A. P. Pisarevskii and Yu. T. Struchkov, *Russ. J. Inorg. Chem.*, 1995, **40**, 339.
28. R. Papiernik, L. G. Hubert-Pfalzgraf, J. C. Daran and Y. Jeannin, *J. Chem. Soc., Chem. Commun.*, 1990, 695.
29. D. J. Teff, J. C. Huffman and K. G. Caulton, *Inorg. Chem.*, 1996, **35**, 2981; *J. Am. Chem. Soc.*, 1996, **118**, 4030.
30. G. B. Deacon and R. J. Philipps, *Coord. Chem. Rev.*, 1980, **90**, 227.
31. S. Boulmaaz, R. Papiernik, L. G. Hubert-Pfalzgraf and J. C. Daran, *Chem. Mater.*, 1991, **3**, 779.
32. I. Laaziz, A. Larbot, A. Julbe, C. Guizard and L. Cot, *Better Ceramics Through Chemistry V, Mater. Res. Soc. Symp. Proc.*, Pittsburgh, 1992, vol. 271, p. 71; P. Toledano, M. Inn and C. Sanchez, *C.R. Acad. Sci. II*, 1990, **311**, 1161.
33. E. P. Turova, N. I. Kozlova, N. Ya Turova, A. I. Belokon, D. V. Berdyev, V. G. Kessler and Yu. K. Grishin, *Russ. Chem. Bull.*, 1995, **44**, A34.
34. S. Daniele, L. G. Hubert-Pfalzgraf, J. C. Daran and R. Toscano, *Polyhedron*, 1993, **12**, 2091.
35. S. Doeuff, Y. Dromzee, F. Taulelle and C. Sanchez, *Inorg. Chem.*, 1989, **28**, 4439.
36. S. P. Faure, P. Barboux, P. Gaucher and J. Livage, *J. Mater. Chem.*, 1992, **2**, 713.
37. R. Kulhman, B. A. Vaarstra, W. E. Streib, J. C. Huffman and K. G. Caulton, *Inorg. Chem.*, 1993, **32**, 1272.
38. R. Papiernik, L. G. Hubert-Pfalzgraf and F. Chaput, *J. Non-Cryst. Solids*, 1992, **147/148**, 36.
39. T. Fukui, C. Sakurai and M. Okuyama, *J. Mater. Res.*, 1992, **7**, 791.
40. S. C. Goel, P. C. Chiang, A. T. Gibbons and W. E. Buhro, '*Better Ceramics Through Chemistry V, Mater. Res. Soc. Symp. Proc.*, Pittsburgh, 1992, vol. 271, p. 3.
41. F. Weiss and L. G. Hubert-Pfalzgraf, to be published.

Paper 6/05266E; *Received* 29th *July* 1996